

## Total cross sections for electron scattering by polyatomic molecules at 10–1000 eV: H<sub>2</sub>S, SiH<sub>4</sub>, CH<sub>4</sub>, CF<sub>4</sub>, CCl<sub>4</sub>, SF<sub>6</sub>, C<sub>2</sub>H<sub>4</sub>, CCl<sub>3</sub>F, CClF<sub>3</sub>, and CCl<sub>2</sub>F<sub>2</sub>

Yuhai Jiang, Jinfeng Sun, and Linde Wan

*Department of Physics, Henan Normal University, Xinxiang, Henan 153002, People's Republic of China*

(Received 20 October 1994)

A model complex optical potential (composed of static, exchange, polarization, and absorption terms) is employed to calculate the total (elastic and inelastic) electron-atom scattering cross sections from the corresponding atomic wave function at the Hartree-Fock level. The total cross sections for electron scattering by their corresponding molecules (H<sub>2</sub>S, SiH<sub>4</sub>, CH<sub>4</sub>, CF<sub>4</sub>, CCl<sub>4</sub>, SF<sub>6</sub>, C<sub>2</sub>H<sub>4</sub>, CCl<sub>3</sub>F, CClF<sub>3</sub>, and CCl<sub>2</sub>F<sub>2</sub>) are obtained by the use of the additivity rule over an incident energy range of 10–1000 eV. The qualitative molecular results are compared with experimental data and other calculations wherever available; good agreement is obtained in intermediate- and high-energy regions.

PACS number(s): 34.80.Bm

### I. INTRODUCTION

The total cross sections (TCSs) for electron scattering by polyatomic molecules (H<sub>2</sub>S, SiH<sub>4</sub>, CH<sub>4</sub>, CF<sub>4</sub>, CCl<sub>4</sub>, SF<sub>6</sub>, C<sub>2</sub>H<sub>4</sub>, CCl<sub>3</sub>F, CClF<sub>3</sub>, and CCl<sub>2</sub>F<sub>2</sub>) have important applications in space, plasma, laser, atmospheric, and chemistry physics [1,2]. Large-scale use of these molecules for halogenated methanes has been made in refrigeration machines, in the manufacture of plastic foams, as propeller gases, and in the semiconductor industry [3]. It is well known that electron-molecule scattering presents a more complex problem than that corresponding to electron-atom scattering due to the multicenter nature, the lack of a center of symmetry (in the case of polyatomic and heteronuclear molecules), and the electron's nuclear motion. Many approaches have been proposed and developed. Here we are interested in the intermediate- and the high-energy regions, where almost all inelastic channels (rotational, vibrational, and electronic excitation, ionization processes, etc.) are open. In this energy range, a conventional close-coupling theory [4–6] for electron-molecule scattering is an arduous task and almost impossible to carry out. It is therefore not surprising that many previous calculations on the TCS for electron-molecule scattering have been restricted to the low-energy region. The spherical complex optical potential (SCOP) model approach has been employed by Jain and co-workers [7,8] to give a summary for H<sub>2</sub>S, SiH<sub>4</sub>, CH<sub>4</sub>, and CF<sub>4</sub> molecules in intermediate- and high-energy regions. The SCOP model is calculated for each collision system from the corresponding molecular wave function at the Hartree-Fock level. For CCl<sub>4</sub>, SF<sub>6</sub>, C<sub>2</sub>H<sub>4</sub>, CCl<sub>3</sub>F, CClF<sub>3</sub>, and CCl<sub>2</sub>F<sub>2</sub> molecules, no calculations are found for the TCS in the present energy region.

A fairly simple approach, namely, the additivity rule [9], was employed successfully by Mark and co-workers [10] to obtain the electron-impact total-ionization cross sections for a variety of molecules. Raj [11] made an application of the additivity rule to obtain the elastic cross sections for electron scattering by a sample of four mole-

cules, namely, O<sub>2</sub>, CO, CO<sub>2</sub>, and CF<sub>4</sub>, at 100–500 eV. Recently Joshipura and Patel [12] also employed the additivity rule and the complex optical potential to obtain the TCS for electron scattering with molecules (O<sub>2</sub>, N<sub>2</sub>, CO, CO<sub>2</sub>) at 100–1000 eV. Very recently we [13] also gave the TCS for electron-molecule (O<sub>2</sub>, N<sub>2</sub>, CO, CO<sub>2</sub>) scattering by the use of the additivity rule and the complex optical potential at 10–800 eV and proved that the additivity rule is proper for the calculation of the TCS for electron-molecule scattering in the intermediate- to high-energy range. In this paper, we further employ the additivity rule and the complex optical potential to obtain the TCS for electron scattering by more complex molecules (H<sub>2</sub>S, SiH<sub>4</sub>, CH<sub>4</sub>, CF<sub>4</sub>, CCl<sub>4</sub>, SF<sub>6</sub>, C<sub>2</sub>H<sub>4</sub>, CCl<sub>3</sub>F, CClF<sub>3</sub>, and CCl<sub>2</sub>F<sub>2</sub>) at 10–1000 eV.

In other experiments, Szymtkowski and Maciag [14], Zecca *et al.* [15–17], Sueoka and co-workers [18,19], Jones [20], Dababneh *et al.* [21], and Floeder *et al.* [22] have measured the TCS in the laboratory for electron scattering from H<sub>2</sub>S, SiH<sub>4</sub>, CH<sub>4</sub>, CF<sub>4</sub>, CCl<sub>4</sub>, SF<sub>6</sub>, C<sub>2</sub>H<sub>4</sub>, CCl<sub>3</sub>F, CClF<sub>3</sub>, and CCl<sub>2</sub>F<sub>2</sub> molecules in different energy ranges.

In the next section we describe in detail the additivity rule and the complex optical potential model. In Sec. III we present the calculations for the TCS on these molecules at 10–1000 eV based on the additivity rule and compared them with the available experimental data. Concluding remarks are made in Sec. IV. We employ atomic units throughout this paper.

### II. THE ADDITIVITY RULE AND COMPLEX OPTICAL POTENTIAL

The basic philosophy of the additivity rule is based on the assumption that anisotropic electron-molecule interactions do not play a significant role in shaping the TCS of the intermediate- and high-energy electron-molecule collisions. According to the additivity rule and the optical theorem [9], the TCS (elastic and inelastic)  $Q_T(E)$  of the molecules is given by

$$\begin{aligned} Q_T(E) &= \frac{4\pi}{k} \text{Im} F_m(\theta=0) = \frac{4\pi}{k} \text{Im} \sum_{j=1}^N f_j(\theta=0) \\ &= \sum_{j=1}^N q_T^j(E) \quad (\text{the additivity rule}), \end{aligned} \quad (1)$$

where  $q_T^j(E)$  and  $f_j$  are the TCS due to the  $j$ th atom of the molecule and the complex scattering amplitude for constituent atoms of the molecule, respectively. Here it is obvious that no molecular geometry is involved in the additivity rule. So the molecular scattering problem is reduced to the atomic scattering problem, which is easier to handle.

In the present investigation the atoms of a molecule are replaced by the appropriate complex optical potential

$$V_{\text{opt}}(r) = V_s(r) + V_e(r) + V_p(r) + iV_a(r). \quad (2)$$

Thus  $V_{\text{opt}}(r)$  incorporates all the important physical effects. Presently the static potential ( $V_s$ ) for electron-atom systems is calculated by using the atomic charge density, determined from the well-known Hartree-Fock atomic wave functions [23]. The exchange potential  $V_e(r)$  provides a semiclassical energy-dependent form derived by Riley and Truhlar [24].

Zhang, Sun, and Liu [25] give a smooth form at all  $r$  for the polarization potential  $V_p(r)$ , which has a correct asymptotic form  $-\alpha/2r^4$  at large  $r$  and approaches the free-electron-gas correlation energy  $V_{\text{co}}(r)$  proposed by Perdew and Zunger [26] in the near-target region

$$V_p(r) = -\frac{\alpha}{2(r^2 + r_{\text{co}}^2)^2}, \quad (3)$$

where the constant  $r_{\text{co}}$  can be determined by letting  $V_p(0) = -\alpha/2r_{\text{co}}^4 = V_{\text{co}}(r=0)$  and  $\alpha$  is the atomic polarizability. This potential model has proved to be fairly successful in obtaining the TCS for electron-atom scattering [25].

The imaginary part of the optical potential  $V_a$  is the absorption potential, which represents approximately the combined effect of all the inelastic channels. Here we employ a semiempirical absorption potential as discussed by Staszewska *et al.* [27]. The  $V_a$  is a function of atomic charge density, incident electron energy, and mean excitation energy  $\Delta$  of the target. It is written as [27]

$$\begin{aligned} V_a(r) &= -\rho(r)(T_L/2)^{1/2}(8\pi/5k^2k_f^3) \\ &\quad \times H(k^2 - k_f^2 - 2\Delta)(A + B + C), \end{aligned} \quad (4)$$

where

$$\begin{aligned} T_L &= k^2 - V_s - V_e - V_p, \\ A &= 5k_f^3/2\Delta, \\ B &= -k_f^3(5k^2 - 3k_f^2)/(k^2 - k_f^2)^2, \\ C &= 2H(2k_f^2 + 2\Delta - k^2) \frac{(2k_f^2 + 2\Delta - k^2)^{5/2}}{(k^2 - k_f^2)^2}, \end{aligned}$$

and  $k^2$  and  $k_f$  are the energy of the incident electron and the Fermi momentum, respectively. Here  $H(x)$  is a Heaviside function defined by  $H(x) = 1$  for  $x \geq 0$  and

$H(x) = 0$  for  $x < 0$ . The absorption potential ( $V_a$ ) has been widely employed to calculate inelastic cross sections for electron-atom [28] and electron-molecule [7,8] scattering.

$q_T^j(E)$  is obtained by the method of partial waves [29]:

$$\begin{aligned} q_T^j(E) &= q_e^j(E) + q_a^j(E) \\ &= \frac{\pi}{k^2} \sum_{l=0}^{l_{\text{max}}} (2l+1) [ |1 - S_l^j|^2 + (1 - |S_l^j|^2) ], \end{aligned} \quad (5)$$

where  $q_e^j(E)$  and  $q_a^j(E)$  are elastic and absorption cross sections, respectively, and  $S_l^j$  is the  $l$ th complex scattering matrix element of the  $j$ th atom, which is related to the partial-wave phase shift as  $S_l^j = \exp(2i\delta_{lj})$ . To obtain  $S_l^j$ , we solve the radial equation

$$\left[ \frac{d^2}{dr^2} + k^2 - V_{\text{opt}} - \frac{l(l+1)}{r^2} \right] u_l(r) = 0 \quad (6)$$

under the boundary condition

$$u_l(kr) \sim kr [j_l(kr) - in_l(kr)] + S_l^j kr [j_l(kr) + in_l(kr)], \quad (7)$$

where  $j_l$  and  $n_l$  are the spherical Bessel and the Neumann function, respectively. The limit  $l_{\text{max}}$  of Eq. (4) is taken to be 50. An effective-range formula

$$\tan \delta_l = -\frac{\pi \alpha k^2}{(2l+1)(2l+3)(2l-1)} \quad (8)$$

is used to generate the higher partial-wave contributions until again a convergence of less than 0.5% is achieved in the TCS. For electron-atom scattering, the complex optical potential can present qualitatively good results for the TCS [25,28] compared with the experimental data and different  $V_e$  and  $V_p$  have smaller effects (within 5%) [12,13] on the TCS in the intermediate- and the high-energy ranges.

### III. RESULTS AND DISCUSSIONS

In Ref [13] we obtained the TCS for electron-molecule ( $\text{O}_2$ ,  $\text{N}_2$ ,  $\text{CO}$ , and  $\text{CO}_2$ ) scattering by employing the additivity rule and the complex optical potential. In this paper, the TCS for the electron-molecule ( $\text{H}_2\text{S}$ ,  $\text{SiH}_4$ ,  $\text{CH}_4$ ,  $\text{CF}_4$ ,  $\text{CCl}_4$ ,  $\text{SF}_6$ ,  $\text{C}_2\text{H}_4$ ,  $\text{CCl}_3\text{F}$ ,  $\text{CClF}_3$ , and  $\text{CCl}_2\text{F}_2$ ) scattering using the additivity rule [Eq. (1)] with  $V_{\text{opt}}$  is calculated in incident energy range 10–1000 eV. In Table I we list the data of atomic TCSs for electron scattering and their molecular TCSs resulting from the use of the additivity rule and the complex optical potential. The present results, along with the available experimental data and the SCOP results of Jain and co-workers [7,8], are shown in Figs. 1–10.

From Fig. 1 we notice that the present values of the TCS resulting from the use of the additivity rule and the SCOP results are in agreement and are lower by about 10% than the measurements of Zecca, Karwasz, and Brusa [16] above 200 eV. However, below 100 eV, the two theoretical calculations agree well with the available measurements [14,16]. As shown in Figs. 2–4, the exper-

TABLE I. Total cross sections for electron scattering by atoms (using a complex optical potential) and their molecules (using the additivity rule) (in units of  $\pi a_0^2$ ).

$E$ (eV)	H	C	F	Si	S	Cl	H <sub>2</sub> S	SiH <sub>4</sub>	CH <sub>4</sub>	CF <sub>4</sub>	CCl <sub>4</sub>	SF <sub>6</sub>	C <sub>2</sub> H <sub>4</sub>	CCl <sub>3</sub> F	CCl <sub>2</sub> F <sub>2</sub>	
10	6.815	16.815	5.943	46.385	40.37	29.858	54.00	73.65	44.08	40.59	136.25	76.03	60.89	112.33	64.50	88.42
20	4.047	13.753	6.069	30.876	25.887	24.811	33.98	47.06	29.94	38.03	113.0	62.30	43.69	94.26	56.77	75.51
30	3.406	12.079	5.952	22.728	19.436	18.474	26.25	36.35	25.70	35.89	85.98	55.15	37.78	73.45	48.41	60.93
49	2.978	10.803	5.723	19.461	16.293	15.310	22.15	31.37	22.72	33.70	72.04	50.53	33.51	62.46	43.28	52.87
50	2.630	9.733	5.466	17.504	14.034	13.407	19.29	28.02	20.25	31.60	63.36	46.83	29.99	55.42	39.54	47.48
60	2.344	8.766	5.217	16.064	12.379	12.027	17.07	25.44	18.14	29.60	56.87	43.62	26.91	50.06	36.44	43.25
70	2.016	7.983	4.983	14.908	11.42	10.846	15.63	23.33	16.41	27.92	51.37	41.32	24.39	45.51	33.78	39.64
80	1.907	7.414	4.767	13.941	10.72	9.882	14.53	21.57	15.04	26.48	46.94	39.32	22.46	41.83	31.6	36.71
90	1.741	6.945	4.573	13.118	10.16	9.197	13.64	20.08	13.91	25.24	43.73	37.60	20.85	39.11	29.86	34.49
100	1.600	6.573	4.392	12.381	9.703	8.698	12.9	18.78	12.97	24.14	41.37	36.06	19.55	37.06	28.45	32.75
200	0.873	4.390	3.157	8.244	6.868	6.148	8.62	11.74	7.88	17.02	28.98	25.81	12.27	25.99	20.01	23.0
300	0.593	3.342	2.468	6.298	5.444	4.902	6.63	8.67	5.71	13.21	22.95	21.52	9.06	20.52	15.70	18.12
400	0.443	2.712	2.081	5.156	4.492	4.140	5.38	6.93	4.48	11.04	19.27	16.98	7.20	17.21	13.10	15.15
500	0.349	2.261	1.801	4.111	3.850	3.513	4.55	5.81	3.66	9.48	16.44	14.67	5.92	14.70	11.22	12.96
600	0.285	1.941	1.588	3.830	3.34	3.120	3.91	4.97	3.08	8.29	14.42	12.87	5.02	12.89	9.83	11.36
700	0.240	1.694	1.429	3.320	2.960	2.800	3.44	4.28	2.65	7.41	12.89	11.54	4.35	11.52	8.78	10.15
800	0.210	1.483	1.292	3.104	2.630	2.470	3.05	3.95	2.32	6.65	11.36	10.38	3.81	10.19	7.83	9.01
900	0.203	1.33	1.184	2.720	2.40	2.230	2.81	3.53	2.14	6.07	10.25	9.51	3.47	9.204	7.11	8.16
1000	0.198	1.22	1.10	2.150	2.10	2.03	2.50	3.21	2.01	5.62	9.34	8.70	2.84	8.41	6.55	7.48

imental data from Zecca *et al.* [15–17], Dababneh *et al.* [21], Jones [20], and Sueoka and co-workers [18,19] exhibit larger discrepancies. The measurements of Sueoka and co-workers are about 15–20 % lower than the other measurements. For SiH<sub>4</sub>, CH<sub>4</sub>, and CF<sub>4</sub> molecules, the present results are in good agreement with the measurements of Zecca *et al.* and Dababneh *et al.* and 10–30 % higher than the data of Sueoka and co-workers above 100 eV. The SCOP results for SiH<sub>4</sub> and CH<sub>4</sub> are about 10% lower than the present results and the available experimental data above 100 eV. For CF<sub>4</sub>, the SCOP results, the present results, and the experimental data are in accord above 100 eV; on the other hand, the SCOP results and the present results substantially exceed the experimental values [16–20] below 100 eV in Figs. 2 and 4. For CH<sub>4</sub> at low energies, the SCOP results are lower than the available experimental data [19,21].

In Figs. 5–10 no other theoretical calculations are found and we report calculations on the TCS for electron scattering for SF<sub>6</sub>, C<sub>2</sub>H<sub>4</sub>, CCl<sub>4</sub>, CCl<sub>3</sub>F, CClF<sub>3</sub>, and CCl<sub>2</sub>F<sub>2</sub> at 10–1000 eV. For SF<sub>6</sub> and C<sub>2</sub>H<sub>4</sub> molecules, as evidenced in Figs. 5 and 6, the present TCS values are 10–25 % higher than the experimental data [19,21,22] in the 100–400 eV range. The measurements of Zecca, Karwasz, and Brusa [16,17] are 15–20 % higher than Sueoka and co-workers' measurements in the present energy range. From Figs. 1–4, the present results show good agreement with the data of Zecca, Karwasz, and Brusa above 100 eV. For SF<sub>6</sub> and C<sub>2</sub>H<sub>4</sub> molecules, Zecca *et al.* do not present experimental data and we assume that our results are within experimental error above 100 eV and that there is much room for possible improvement on the experimental values.

The present TCS results show good agreement with the experimental data of Zecca, Karwasz, and Brusa [17] at

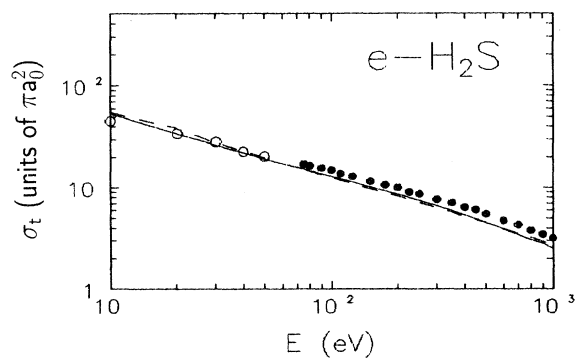


FIG. 1. Total cross sections for  $e$ -H<sub>2</sub>S scattering. Solid curve, present results; dashed curve, SCOP results [7]. The experimental data:  $\circ$ , Ref. [14];  $\bullet$ , Ref. [16].

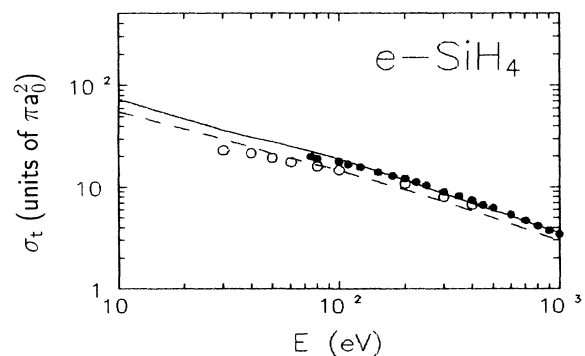


FIG. 2. Same as in Fig. 1, but for SiH<sub>4</sub>. The experimental data:  $\circ$ , Ref. [18];  $\bullet$ , Ref. [16].

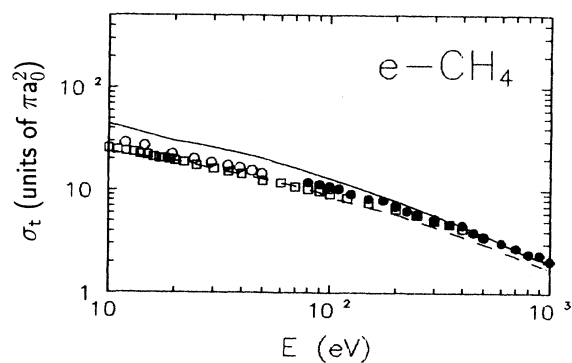


FIG. 3. Same as in Fig. 1, but for  $\text{CH}_4$ . The experimental data:  $\circ$ , Ref. [21];  $\bullet$ , Ref. [15];  $\square$ , Ref. [19].

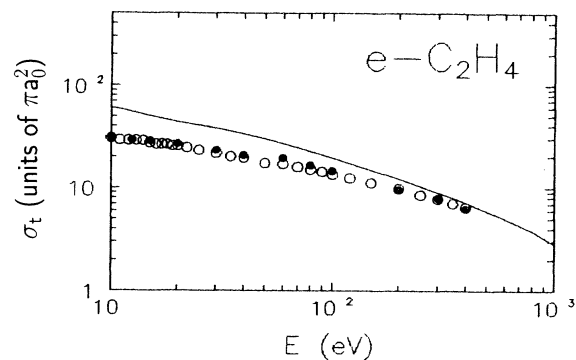


FIG. 6. Same as in Fig. 5, but for  $\text{C}_2\text{H}_4$ . The experimental data:  $\circ$ , Ref. [19];  $\bullet$ , Ref. [22].

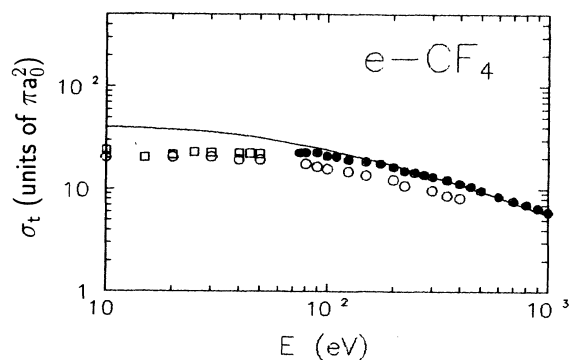


FIG. 4. Same as in Fig. 1, but for  $\text{CF}_4$ . The experimental data:  $\circ$ , Ref. [18];  $\bullet$ , Ref. [17];  $\square$ , Ref. [20].

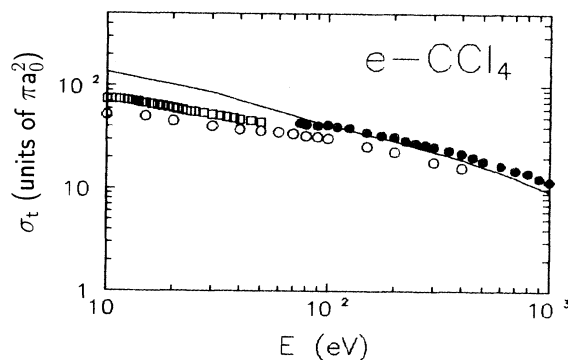


FIG. 7. Same as in Fig. 5, but for  $\text{CCl}_4$ . The experimental data:  $\circ$ , Ref. [18];  $\bullet$ , Ref. [17];  $\square$ , Ref. [20].

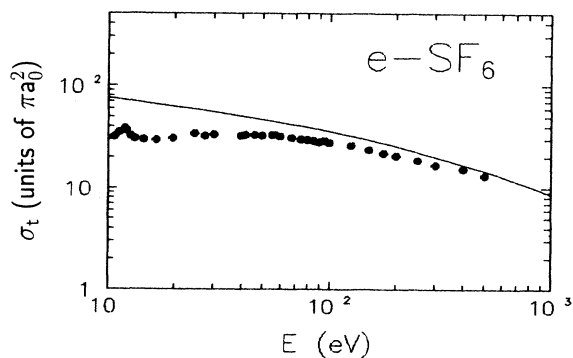


FIG. 5. Total cross sections for  $e\text{-SF}_6$  scattering. Solid curve, present results. The experimental data:  $\bullet$ , Ref. [21].

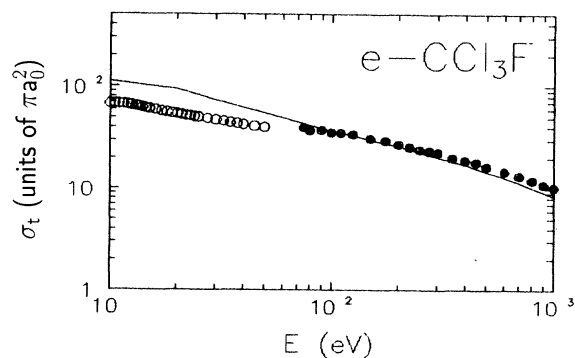
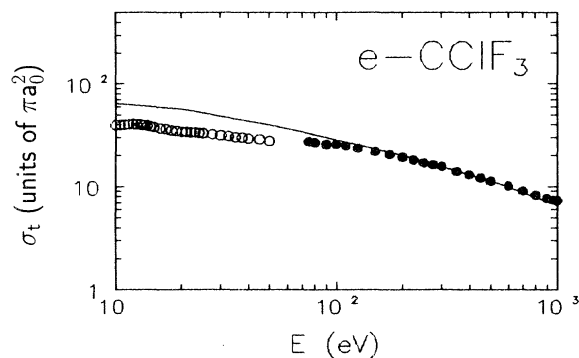
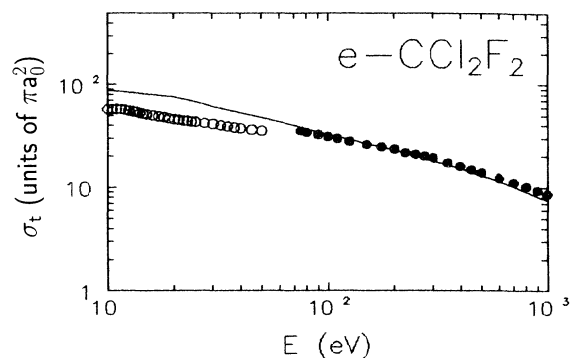


FIG. 8. Same as in Fig. 5, but for  $\text{CCl}_3\text{F}$ . The experimental data:  $\circ$ , Ref. [20];  $\bullet$ , Ref. [17].

FIG. 9. Same as in Fig. 8, but for  $\text{CClF}_3$ .FIG. 10. Same as in Fig. 8, but for  $\text{CCl}_2\text{F}_2$ .

all the overlap energies in Figs. 7–10. For  $\text{CCl}_4$ , as shown in Fig. 7, the measurements of Mori, Katayama, and Sueoka [18] are 20–30% lower than the two other groups of experimental data [17,20] and our results at the present energy range. For  $\text{CCl}_4$ ,  $\text{CCl}_3\text{F}$ ,  $\text{CClF}_3$ , and  $\text{CCl}_2\text{F}_2$  chlorofluoromethanes, at 700–1000 eV, the present results are 10–20% lower than the experimental data. According to the analysis of Zecca, Karwasz, and Brusa, for these gases, longer evacuation times were necessary and statistical fluctuations affected their data to a greater extent (about 3%). So our results also are in agreement with the experimental data above 100 eV. In the low-energy range, our results are about 30–50% higher than the measurements of Jones [20] for  $\text{CCl}_4$ ,  $\text{CCl}_3\text{F}$ ,  $\text{CClF}_3$ , and  $\text{CCl}_2\text{F}_2$ .

As the energy of the incident electron increases, the interactions among the atoms of a molecule have a smaller effect on the TCS. The additivity rule ignores the interactions, so we see, from Figs. 1–10, that the present approach is in fairly good agreement with the available experimental data in the intermediate- and the high-energy ranges; however, at low energies, our results are not as good.

#### IV. CONCLUSIONS

The additivity rule ignores molecular geometry, so the molecular scattering problem is reduced to the atomic scattering problem, which is easier to handle. Joshipura

and Patel [12] and Sun, Jiang, and Wan [13] recently calculated the TCS for electron scattering from diatomic and triatomic molecules using the additivity rule and obtained good results in the intermediate- and the high-energy ranges. In this paper we employ the additivity rule and obtain quite encouraging results for the TCS on more complex  $\text{H}_2\text{S}$ ,  $\text{SiH}_4$ ,  $\text{CH}_4$ ,  $\text{CF}_4$ ,  $\text{CCl}_4$ ,  $\text{SF}_6$ ,  $\text{C}_2\text{H}_4$ ,  $\text{CCl}_3\text{F}$ ,  $\text{CClF}_3$ , and  $\text{CCl}_2\text{F}_2$  molecules. Even though the mathematical calculations are not exact, the present results provide a good qualitative comparison and a basis for future experimental research, particularly for those molecules for which the wave functions, without which many theoretical calculations cannot be done, are not currently available. So the additivity rule and the optical potential model of related atoms are used to calculate qualitatively the TCS for electron-molecule scattering in the intermediate- and the high-energy ranges. The additivity rule provides insight into the calculations of the TCS of electron-molecule scattering and is of value for further research. At the same time, we notice large differences among the experimental data and hope that improved experiments will elicit more accurate results. Since the contribution from the interference occurring between the scattering amplitudes originating from the different constituent atoms of the molecule is not included in the additivity rule, the results of the TCS using the additivity rule show larger discrepancies in the low-energy range.

- [1] *Electron Molecule Interactions and Their Applications*, edited by L. G. Christophorou (Academic, New York, 1984), Vols. 1 and 2.
- [2] *Molecular Processes in Space*, edited by T. Watanabe *et al.* (Plenum, New York, 1990).
- [3] J. W. Butterbough, D. C. Gray, and H. H. Sawin, *J. Vac. Sci. Technol. B* **9**, 1461 (1991).
- [4] N. F. Lane, *Rev. Mod. Phys.* **29**, 40 (1980).
- [5] *Electron-Atom and Electron-Molecule Collisions*, edited by J. Hinze (Plenum, New York, 1983).
- [6] *Aspects of Electron-Molecule Scattering and Photoionization*, edited by Arvid Herzenberg, AIP Conf. Proc. No.

- 204 (AIP, New York, 1990).
- [7] A. Jain and K. L. Baluja, *Phys. Rev. A* **45**, 202 (1992).
- [8] K. L. Baluja, A. Jain, V. Di. Martino, and F. A. Gianturco, *Europhys. Lett.* **17**, 139 (1992).
- [9] J. W. Otvos and D. P. Stevenson, *J. Am. Chem. Soc.* **78**, 546 (1956); W. L. Fitch and A. D. Sauter, *Anal. Chem.* **55**, 832 (1983).
- [10] D. Margreiter, H. Deutsch, M. Schmidt, and T. D. Mark, *Int. J. Mass Spectrom. Ion Processes* **100**, 157 (1990); H. Deutsch, D. Margreiter, and T. D. Mark, *ibid.* **93**, 259 (1989).
- [11] D. Raj, *Phys. Lett. A* **160**, 571 (1991).

- [12] K. N. Joshipura and P. M. Patel, *Z. Phys. D* **29**, 269 (1994).
- [13] Jinfeng Sun, Yuhai Jiang, and Linde Wan, *Phys. Lett. A* **195**, 81 (1994).
- [14] C. Szmytkowski and K. Maciag, *Chem. Phys. Lett.* **129**, 321 (1986).
- [15] A. Zecca, G. Karwasz, R. S. Brusa, and R. Grisenti, *J. Phys. B* **23**, 2737 (1991).
- [16] A. Zecca, G. Karwasz, and R. S. Brusa, *Phys. Rev. A* **45**, 2777 (1992).
- [17] A. Zecca, G. Karwasz, and R. S. Brusa, *Phys. Rev. A* **46**, 3877 (1992).
- [18] S. Mori, Y. Katayama, and O. Sueoka, *At. Coll. Res. Jpn.* **11**, 19 (1985).
- [19] O. Sueoka and S. Mori, *J. Phys. B* **19**, 4035 (1986).
- [20] R. K. Jones, *J. Chem. Phys.* **84**, 813 (1986).
- [21] M. S. Dababneh, Y. F. Hsieh, W. E. Kauppila, Ch. K. Kwan, S. J. Smith, T. S. Stein, and M. N. Uddin, *Phys. Rev. A* **38**, 1207 (1988).
- [22] K. Floeder, D. Fromme, W. Raith, A. Schuab, and G. Sinapius, *J. Phys. B* **18**, 3347 (1985).
- [23] E. Clementi and C. Roetti, *At. Data Nucl. Data Tables* **14**, 177 (1974).
- [24] M. E. Riley and D. G. Truhlar, *J. Chem. Phys.* **63**, 2182 (1975).
- [25] X. Z. Zhang, J. F. Sun, and Y. F. Liu, *J. Phys. B* **25**, 1893 (1992).
- [26] J. P. Perdew and A. Zunger, *Phys. Rev. B* **23**, 5048 (1981).
- [27] G. Staszewska, D. W. Schwenke, D. Thirumalai, and D. G. Truhlar, *Phys. Rev. A* **28**, 2740 (1983).
- [28] S. N. Nahar and J. M. Wadehra, *Phys. Rev. A* **43**, 1275 (1991).
- [29] *The Optical Model of Elastic Scattering*, edited by P. E. Hodgson (Oxford University Press, New York, 1963).